Journal of Power Sources 246 (2014) 423–429

Contents lists available at ScienceDirect

Journal of Power Sources

journal homepage: www.elsevier.com/locate/jpowsour

Long-term room-temperature hydrazine/air fuel cells based on low-cost *nanotextured* Cu–Ni catalysts

Boris Filanovsky [a,1], Eran Granot [a,1], Igor Presman [b], Iliya Kuras [b], Fernando Patolsky [a,*]

[a] School of Chemistry, The Raymond and Beverly Sackler Faculty of Exact Sciences, Tel-Aviv University, Tel-Aviv 69978, Israel
[b] Nanergy, Ltd., Hertzeliya, Israel

HIGHLIGHTS

- A novel *nanotextured* copper–nickel anode/hydrazine fuel cell device was demonstrated.
- The fuel cell device exhibits long-term stability for continuous operation, up to ~2000 h.
- The new fuel cell makes use of low-cost catalysts and exhibits high electrochemical performances.
- This fuel cell is effectively operated at RT; higher temperatures up to 60 °C improve its efficiency.
- Design optimization is expected to improve its working life, as well as its electrochemical efficiency.

ARTICLE INFO

Article history:
Received 25 January 2013
Received in revised form
8 July 2013
Accepted 23 July 2013
Available online 2 August 2013

Keywords:
Fuel cell
Copper
Nickel
Anode
Hydrazine
Energy

ABSTRACT

We present here a long-term room-temperature (RT) direct-liquid hydrazine/air fuel cell device. This hydrazine/air fuel cell is based on low-cost easily-prepared *nanotextured* Cu–Ni anodes as the hydrazine (Hz) catalyst, combined with a commercial anion-exchange membrane film and a commercial air cathode. In addition, our hydrazine/air fuel cell consists on an improved novel design that results in remarkably high mechanical and chemical stabilities for long periods of operation. This hydrazine/air fuel cell can operates continuously for about ~2000 h (limited mainly by cathode and membrane deterioration) with continuous fuel supply, and supplies about 0.58 V at 1 A (14.3 mA cm^{-2}, with a discharge efficiency of about 70% (drift is less than 0.01% h^{-1}), and appears to be suitable for mass production. The use of optimally-combined multi-metal electrodes suggests the possibility to create novel catalysts of improved electrochemical efficiency and stability. Our fuel cell devices can find broad applications in different civilian and military field mobile and stationary uses, for instance, in future fuel-cell operated vehicles and stationary back-up power electrical stations.

1. Introduction

Fuel cell devices (FC) enable the conversion of the chemical energy stored in a fuel into electrical energy, and are characterized by their high electrochemical energy densities, typically 2–8 kWh kg^{-1}, ten times that of conventional batteries [1]. Many types of fuel cells have been developed over the last decades [1–11]. Among them, low-temperature fuel cells, which operate at high energy density and high efficiency, are considered to be among the most suitable power sources for portable and stationary applications [5,9]. However, until today, due to numerous challenging limitations, mainly related to the limited structural and functional cell stability for long-term periods of continuous operation, there has been no mass deployment of fuel cells devices.

During the last decade, intensive research efforts have been focused on hydrogen-rich fuels such as methanol [12–16], sodium borohydride [1,17–22], ammonia–borane [23–28] and hydrazine [29–43]. Hydrazine is an attractive fuel candidate because of its low cost, abundance and relatively simple synthesis. The natural basic sources of hydrazine, nitrogen and hydrogen, are unlimited and there is no practical recycling limitation. In addition, the decomposition products of hydrazine, nitrogen and water, are ecologically friendly. Pure anhydrous hydrazine (N_2H_4) is considered hazardous and toxic, while dilute hydrazine solutions are substantially less hazardous. Moreover, several hydrazine salt derivatives have been

* Corresponding author.
E-mail address: fernando@post.tau.ac.il (F. Patolsky).
[1] These authors contributed equally.

0378-7753/$ – see front matter © 2013 Elsevier B.V. All rights reserved.
http://dx.doi.org/10.1016/j.jpowsour.2013.07.084

reported as prospective anticancer drugs [44]. Hydrazine was used also as a source of hydrogen for indirect fuel cells [48–50].

Hydrazine-based direct-liquid fuel cells (DLFC) were first developed in the 1960s [29], but only in recent years there have been increased research efforts in this field [30–36] due to the increased cost of oil and growing demand for stationary and mobile applications. However, most of these reported hydrazine-based fuel cells are expensive because of the use of noble metals catalysts. Furthermore, to the best of our knowledge the stability of these fuel cell devices under long-term discharge conditions were not directly demonstrated.

Noble metals such as Pt, Pd, Ru and Rh were suggested as effective catalysts for the electro-oxidation of hydrazine [32,37]. Different metal/carbon matrix combinations such as Ni–Pt/carbon [31], Pt/carbon [34], Ag/carbon-nanotube [38] and graphene–platinum nanocomposites [39] have also been suggested as hydrazine catalysts. However, these metal/carbon compounds are not mechanically stable, particularly at high current densities and high temperatures (above 60 °C), as a result of the formation of gas bubbles. Yi et al. proposed an Ag/Ti substrate as hydrazine catalyst [40]. In this case the electro-oxidation onset potential is about −0.5 V (vs. $-Hg/Hg_2Cl_2$), and the anode supplied a voltage of about −0.4 V at 3 mA cm^{-2}. Nickel and its alloys have also been used as hydrazine electro-oxidation catalysts for fuel cells [31,34,41–43]. For instance, the metal alloy $Ni_{60}Co_{40}$, was suggested as a hydrazine catalyst [41]. In this case, the oxidation of hydrazine occurs at over-potentials of about 300 mV, and the anode catalyst functions for only a short time, about 90 min. Furthermore, Li et al. developed a hydrazine/oxygen fuel cell with the use of a Zr/Ni alloy as the hydrazine catalyst [42]. This fuel cell supplies about 0.5 V at 100 mA cm^{-2} with a supply of pure oxygen (discharge data were not shown). Also, Asazawa et al. developed a hydrazine/oxygen fuel cell with the use of Ni or Co anodes, and an anion-exchange membrane [43]. This fuel cell operated with the use of a supply of pure oxygen at 80 °C (discharge data were not shown). In this study, nickel was found to be the most suitable anode catalyst amongst Co, Ni, and Pt for use in the direct-hydrazine anion-exchange membrane fuel cell, however, data about long-term discharge characteristics of this device were not provided. According to the data presented, nickel and its alloys have great potential as hydrazine catalysts in fuel-cell applications.

In a previous series of studies, we reported that *nanotextured* copper electrodes function as highly efficient, chemically and electrochemically stable catalysts for the electro-oxidation of hydrazine [36,45]. Our Cu/hydrazine anodes showed high electrical efficiency and stability for long periods of continuous electro-oxidation. These *nanotextured* copper electrodes were used successfully in the construction of a preliminary hydrazine/air fuel cell device.

Here, we present the latest advancements in the development of our hydrazine/air fuel cell devices, which result in substantially increased operation times of near ~2000 h. Our hydrazine/air fuel cell is based on novel *nanotextured* bimetallic Cu–Ni foam as the hydrazine catalyst, combined with a commercial anion-exchange membrane film and commercial air cathode. In addition, improvement in the construction design of the cell resulted in substantially increased stability and operation times, as a result of lower hydrazine cross-over, and thus lower hydrazine concentration on the cathode's side, and the rapid evacuation of gas bubbles from the cathode compartment. This improved fuel cell assembly operated continuously for nearly 2000 h, with continuous fuel supply. The cell supplies about 0.58 V at 1 A (14.3 mA cm^{-2}), and the discharge efficiency of hydrazine corresponds to about 70% (drift less than 0.01% h^{-1}). The use of optimally-combined bimetallic Cu–Ni anode electrodes was demonstrated to lead to anodes of improved catalytic properties, along with improved electrochemical efficiency and stability.

2. Experimental

2.1. Materials and equipment

Pure Cu foam (95PPI, 1 mm thick) was purchased from Shanghai Winfay New Material Co., Ltd. Hydrazine hydrate solution (62%) was purchased from Across Chemicals. All other chemical reagents were purchased from Sigma–Aldrich in analytical grade. Anion-exchange-membrane film (28 μm thick) was purchased from Tokuyama Co Japan. Air cathode was purchased from eVionyx Co. (USA). The commercial air-cathode consists of carbon powder, polymer and cobalt porphyrin complex as catalyst.

Ultrapure water ($R = 18$ MΩ, Barnstead Easy-Pure RF) was used in all the experiments. The electrochemical experiments were performed at room temperature (RT) and conducted with a PC-controller (Autolab GPES software version 4.9) and Autolab potentiostat/galvanostat (PGSTAT302N). Electrochemical half-cell measurements were performed in a conventional three-electrode cell comprising the anode working electrode, a reference double junction Ag/AgCl (sat. KCl) electrode (Metrohm, catalog No. 6.0726.100) connected to a Luggin capillary and a high-surface-area carbon (10 × 3.5 mm) counter electrode. The potential of the reference electrode was examined (compared with fresh reference electrode) before and after each experiment and found to be stable in the range of ±10 mV.

Long-discharge measurements of our fuel cell were performed galvanostatically with the use of a Maccor instrument, Maccor Co (USA). The electrodes were imaged by SEM (Jeol, JSM-6700F). UV–Visible spectrometer (spUVS™, model sp-1900) was used for hydrazine concentration monitoring.

2.2. Preparation of Cu–Ni foam catalyst

The Cu foam (1 mm thick) was electroplated (in order to increase its surface area) at 3 A dm^{-2} (RT) for 20 min in a solution containing 1 M $CuSO_4 \cdot 5H_2O$, 1 M H_2SO_4, 50 mM HCl and 20 mM glacial acetic acid (CH_3COOH) [46]. Then, the Cu-foam electrode was once again electroplated at 3 A dm^{-2} (RT) for 240 s in a solution containing 1 M $NiSO_4 \cdot 7H_2O$, 0.12 M $NiCl_2 \cdot 6H_2O$ and 0.5 M H_3BO_3 at pH 5.0 [47], Ni loading is about 1 mg cm^{-2} (geometrical area).

2.3. Fuel-cell measurements

The homemade hydrazine/air fuel cell consists of a 70 cm^2 Cu–Ni foam anode (1 mm thick) and a 70 cm^2 commercial air cathode, combined with a commercial hydroxide-exchange membrane film. This fuel cell was operated under continuous flow (20 mL min^{-1}) of fuel solution (3% hydrazine in 5.5 M KOH). The hydrazine concentration was analyzed every few days and hydrazine was added as needed. The efficiency of the discharge process was calculated according to Equation (1).

$$\eta(\%) = Q_d\ 100/Q_t. \quad (1)$$

where η is the efficiency (reported as a percentage), Q_t is the calculated theoretical charge (in coulombs, corresponding to the total amount of hydrazine) and Q_d is the real charge derived from the discharge curve.

2.4. Hydrazine concentration monitoring

We developed an application for the monitoring of hydrazine concentration of the fuel cell. This application is based on the reaction between 4-dimethylamino-benzaldehyde (Ehrlich's reagent) and hydrazine, resulting in the formation of an imine compound characterized by maximum absorbance at 480 nm. A solution

containing 0.5 mL 0.04 M 4-dimethylamino-benzaldehyde in ethanol (1) was mixed with 80 μL of solution (2), which contains 100 μL of fuel-cell solution (hydrazine in KOH) diluted in 40 mL of water. 20 μL of 30% HCl was added and the solution was stirred for 5 min, then ethanol was added to a total volume of 10 mL.

2.5. Roughness factor determination

Cyclic voltammograms were performed with the use of our untreated Cu foam electrode compared with the *nanotextured* Cu–Ni foam electrode, in non-faradic range (3 M KOH, between −1.2 V to −0.7 V, 100 mV s^{-1}). The ratio between the ΔI_P (A) at E=−0.95 V of the *nanotextured* Cu–Ni foam electrode and the untreated Cu-foam electrode corresponds to the surface area ratio between both electrodes.

3. Results and discussion

In previous studies we revealed that *nanotextured* copper electrodes function as highly efficient and ultra-long-lasting catalysts for the electro-oxidation of amino-derivative fuels, and hydrazine among them [28,36,45]. In this work, Cu foam was used as the anode base material [46], owing to its high surface area, low electrical resistivity, high chemical (electrochemical) stability under alkali conditions, high mechanical stability and its low cost per-metal-weight. Representative SEM (scanning electron microscope) images of our Cu-foam-based anodes are shown in Fig. 1.

In order to further improve the electrochemical properties (OCP, open circuit potential, and discharge potential) of our Cu-foam catalyst towards the catalytic electro-oxidation of hydrazine; its surface area was further increased by electroplating Cu. Furthermore, since Ni and its alloys have been successfully employed as effective hydrazine catalysts [31,34,41–43], our Cu anode (increased-area foam anode) was post-electroplated with controllable amounts of Ni. Preliminary results show that the optimal amount of Ni loading corresponds to about 1 mg cm^{-2}. Higher Ni loadings result in the significantly increased non-electrochemical decomposition of the hydrazine fuel, a process that clearly and dramatically reduces the efficiency of the anode material as a candidate for the electro-oxidation of hydrazine.

The different Cu-foam electrodes were imaged by SEM, as presented in Fig. 2. Clearly, the surface area of the Cu foam electrode (A–B) increased dramatically after Cu electroplating (C–D), and after Ni electroplating (E–F). The Cu electroplated foam catalyst (C–D) as well as the Cu–Ni foam catalyst (E–F) contains large amount of spheres in the range of 100–400 nm. These striking structural and morphological differences between the untreated Cu-foam electrode (A–B) and the Cu–Ni-foam electrode (E–F) are expected to have a major influence on the electrochemical oxidation of hydrazine. The roughness factor difference between the *nanotextured* Cu–Ni foam electrode and the untreated Cu foam electrode corresponds to about 10.

XRD analysis shows the presence of Ni clusters on the respective Cu surfaces as shown in Fig. 3. EDAX measurements show that the amount of Ni on the surface of the Cu–Ni foam corresponds to about 3%.

Fig. 4A presents the hydrazine electro-oxidation performance in alkaline solution of the *nanotextured* Cu–Ni foam catalyst (curve a), compared to the electrochemical performance obtained with the electroplated *nanotextured* Cu-only foam catalyst (curve b) and with the untreated Cu foam catalyst (curve c).

The *nanotextured* Cu–Ni/hydrazine anode shows an OCP (open circuit potential) of about −1.15 V (vs. Ag/AgCl), while the OCP of the electroplated *nanotextured* Cu-only anode (increased surface area) and the untreated Cu-foam smooth anode is about −1.10 V and −1.05 V, respectively. The oxidation current generated by the *nanotextured* Cu–Ni catalyst (curve a) and the electroplated *nanotextured* Cu-only catalyst (curve b) appear at an onset potential above about −1.05 V, while the oxidation current generated by the untreated smooth Cu catalyst (curve c) appears at an onset potential above about −0.95 V. In addition, the oxidation current generated by the Cu–Ni catalyst (curve a) is approximately three times higher than that of the electroplated Cu-only catalyst (curve b), and about 13 times that of the untreated smooth Cu catalyst (curve c) at $E = -0.85$ V (vs. Ag/AgCl). Clearly, the decoration of Cu anodes with only 3% surface nickel leads to a substantial improvement in the measured current density, without negatively affecting the catalyst electrochemical efficiency due to potentially increased non-electrochemical degradation of the hydrazine fuel by the nickel deposited traces. These findings further suggest that a new generation of catalyst may be envisioned by the simple combination of multiple metals in a single electrode. The optimized combination of several metals, each metal contributing its intrinsic advantages, may lead to the formation of catalysts of improved characteristics, while concurrently hindering handicapping weaknesses of certain metal components.

Full discharge (at 0.14 A, 14 mA cm^{-2}) is shown in Fig. 4B. The most negative potential of about −0.98 V (vs. Ag/AgCl) was observed for the *nanotextured* Cu–Ni foam catalyst (curve a), while a potential of about −0.70 V was observed for the *nanotextured* Cu foam catalyst (curve b) and a potential of about −0.55 V was observed for the untreated Cu-foam catalyst (curve c). The *nanotextured* Cu–Ni foam catalyst displays the most negative potential, and a remarkable discharge efficiency of about 94%.

Based on these important results, a hydrazine/air fuel cell was constructed with the use of the Cu–Ni *nanotextured* catalyst, combined with a commercial air cathode, and a commercial anion-exchange-membrane, as shown in Fig. 5A. The classical fuel cells construction, where the membrane is directly attached to the

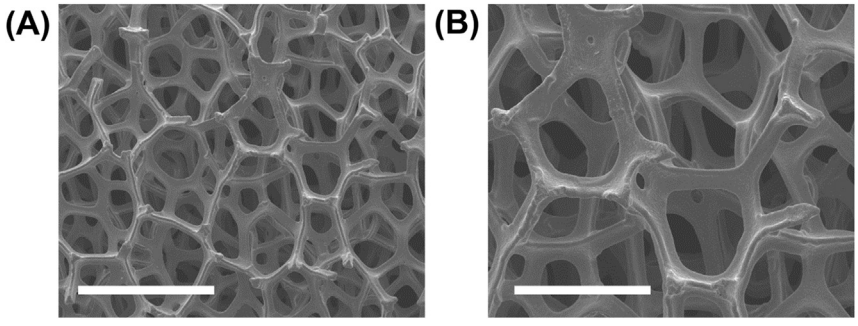

Fig. 1. SEM images of our Cu foam-based anodes. Scale bars for panel (A) is 1 mm, and for panel (B) is 500 μm.

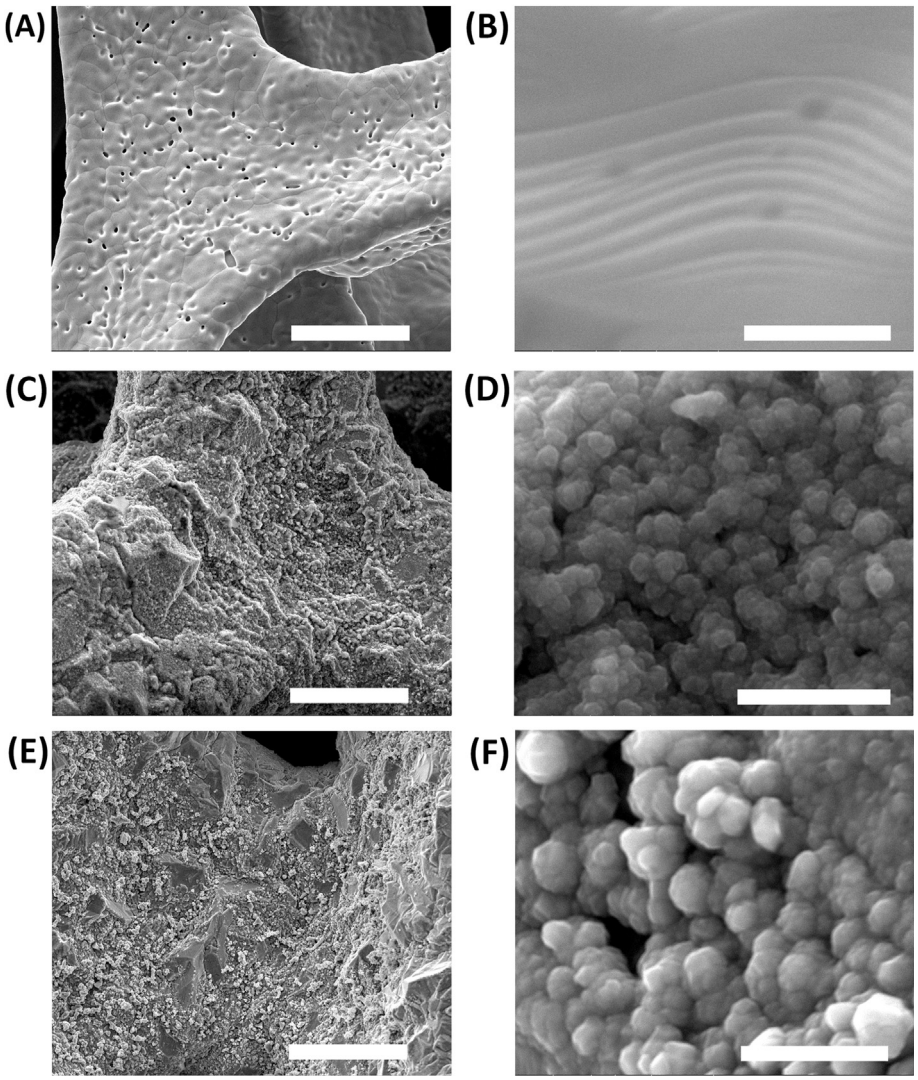

Fig. 2. SEM images of different foam electrodes: (A)–(B) untreated Cu foam, (C)–(D) Cu foam after electroplating of Cu, and (E)–(F) Cu–Ni foam (Cu foam after electroplating of Cu and Ni). Scale bars for A, C and E images are 50 μm, and for B, D and F images are 2 μm.

cathode, was widely used in most fuel cell applications reported in past [34,35,43]. Using this classical construction, the commercial anion-exchange-membrane film was directly glued to the air cathode (by the use of membrane solvent at high temperature, 220 °C). This fuel cell device failed to operate after about 200 h at 1 A (14.3 mA cm^{-2}), with continuous flow of fuel solution. During the discharge process the potential of the Cu–Ni anode was in a range between −1.0 to −0.9 V (vs. Ag/AgCl), while the potential of the air-cathode degraded from about −0.3 V to about −0.9 V (vs. Ag/AgCl), after about 200 h, and the cathode lost almost completely its activity. After a closer inspection, it was found that the membrane detached from the air cathode surface, presumably as a result of the formation of gas bubbles at the interface between the cathode and the membrane (Fig. 5B). The accumulation of bubbles was most probably due to the non-electrochemical decomposition of hydrazine on the air cathode, since hydrazine crosses over from the anodic compartment through the membrane into the cathode surface, resulting in a dramatic and rapid deterioration of the cathode activity. We would like to emphasize that gas bubbles evacuated immediately (when formed) in the anode compartment, because the Cu–Ni foam is not directly attached to the membrane, and in addition, the anodic solution is stirred constantly by the continuous flow of the fuel solution.

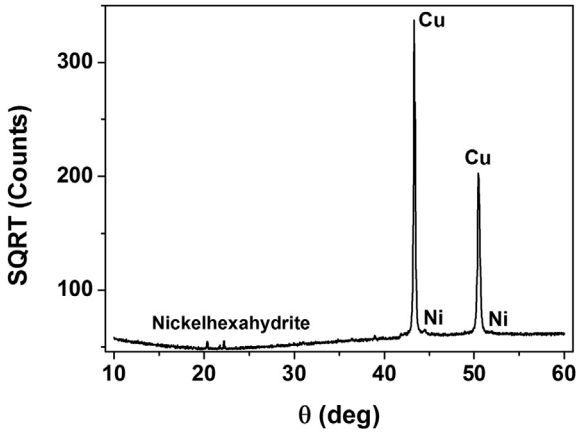

Fig. 3. XRD analysis of a representative Cu–Ni anode.

However, gas bubbles cannot be evacuated from the cathode compartment, when formed on the cathode surface, since the membrane is directly attached (glued to) to the air cathode in this

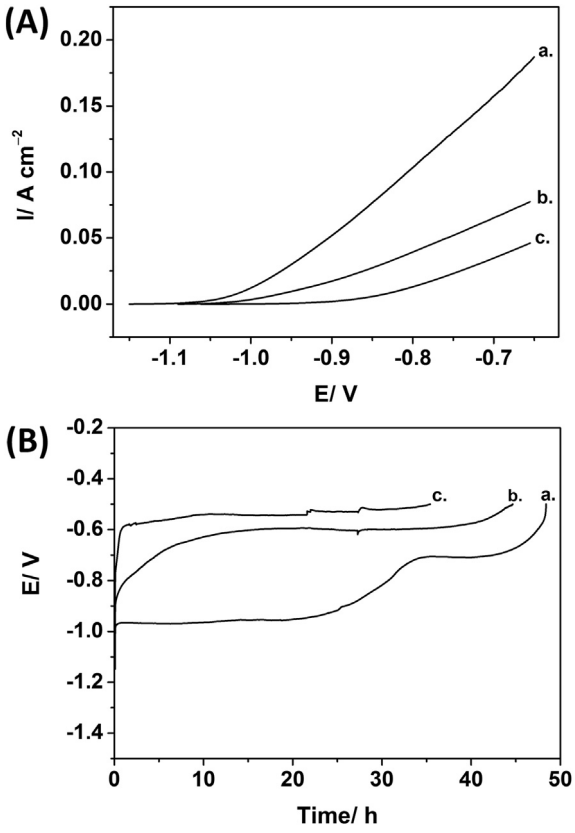

Fig. 4. (A) The electro-oxidation of hydrazine on different catalysts: (a) *nanotextured* Cu–Ni foam, (b) electroplated *nanotextured* Cu-only foam and (c) untreated smooth Cu foam. (B) Anode half-cell discharge at 0.14 A (14 mA cm^{-2}) with the use of different catalysts: (a) *nanotextured* Cu–Ni foam, (b) electroplated *nanotextured* Cu-only foam and (c) untreated smooth Cu foam. Electrode area corresponds to 10 cm^2 in all experiments. The experiments were carried out in 1 M (3%) hydrazine in 6 M KOH (70 mL solution), scan rate 50 mV s^{-1}. Ag/AgCl (sat. KCl) was used as the reference electrode.

construction (Fig. 5). The membrane detaches from the air cathode when gas bubbles accumulate, resulting in a dramatic decrease of the cathode activity. In addition, we found that the air-cathode losses its activity in the presence of high concentrations of hydrazine (above 10%), after only a few hours of operation (even at the OCP regime). Also, the air-cathode losses its activity after 100 h at 14.3 mA cm^{-2}, without the use of the anionic membrane, even at low hydrazine concentrations of 3%.

Furthermore, we found that the cathode lost its activity at high current density, above 100 mA cm^{-2}. However, this air cathode can

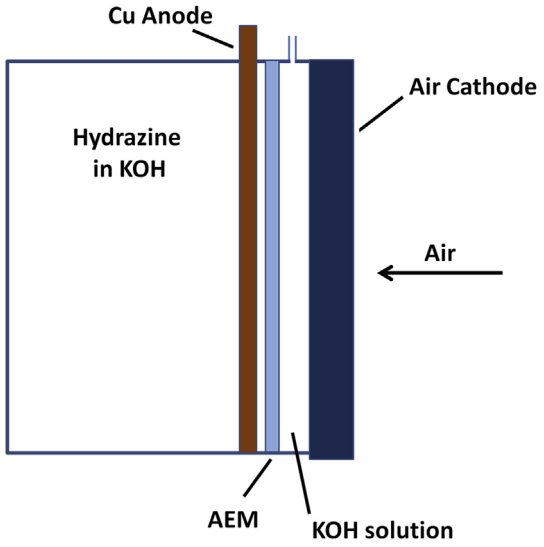

Fig. 6. The new fuel-cell design, displaying the 'buffering' protection chamber.

function properly for long periods of time at a current density of about 20 mA cm^{-2}.

In order to achieve a better reliability and longer operation times, a new cell design was constructed, as shown in Fig. 6. In this design, the anion-exchange-membrane film is separated from the air cathode by a KOH-solution chamber (about 5 mm thick). Here, gas bubbles when formed, cannot become trapped between the membrane and the air cathode. This prevents the excessive accumulation of gas products in the cathode/membrane interface region, and the further detachment of the membrane from the cathode surface. In addition, the concentration of hydrazine near the air cathode surface is dramatically reduced, compared to the previous design as per Fig. 5, since the crossed-over hydrazine from the anodic compartment become largely diluted by the KOH solution in this 'buffering' protection chamber. It is essential to construct this design (Fig. 6) very carefully in order to avoid any tearing of the membrane resulting in penetration of hydrazine inside the air cathode, and thus fast cathode deterioration.

Following this novel design, a new hydrazine/air fuel cell (70 cm^2 surface area, 100 mL volume) was constructed according to Fig. 6. The observed OCP of this fuel cell is about 0.96 V. The resulting *E* vs. *I* curve is shown in Fig. 7A. The *P* vs. *I* curve derived is presented in Fig. 7B. This fuel cell supplies a maximum power of about 0.63 W (9 mW cm^{-2}) at 1.5 A (21.4 mA cm^{-2}). The full-discharge curve at 1 A (14.3 mA cm^{-2}) is shown in Fig. 7C. The

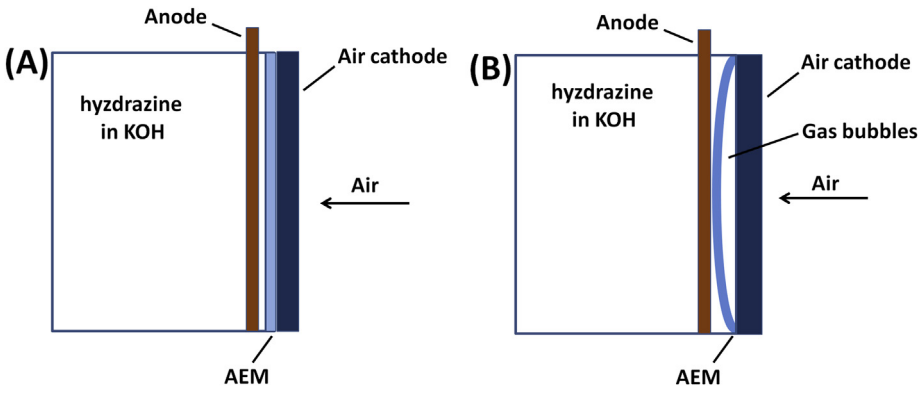

Fig. 5. Fuel-cell device (A) before failure and (B) after failure.

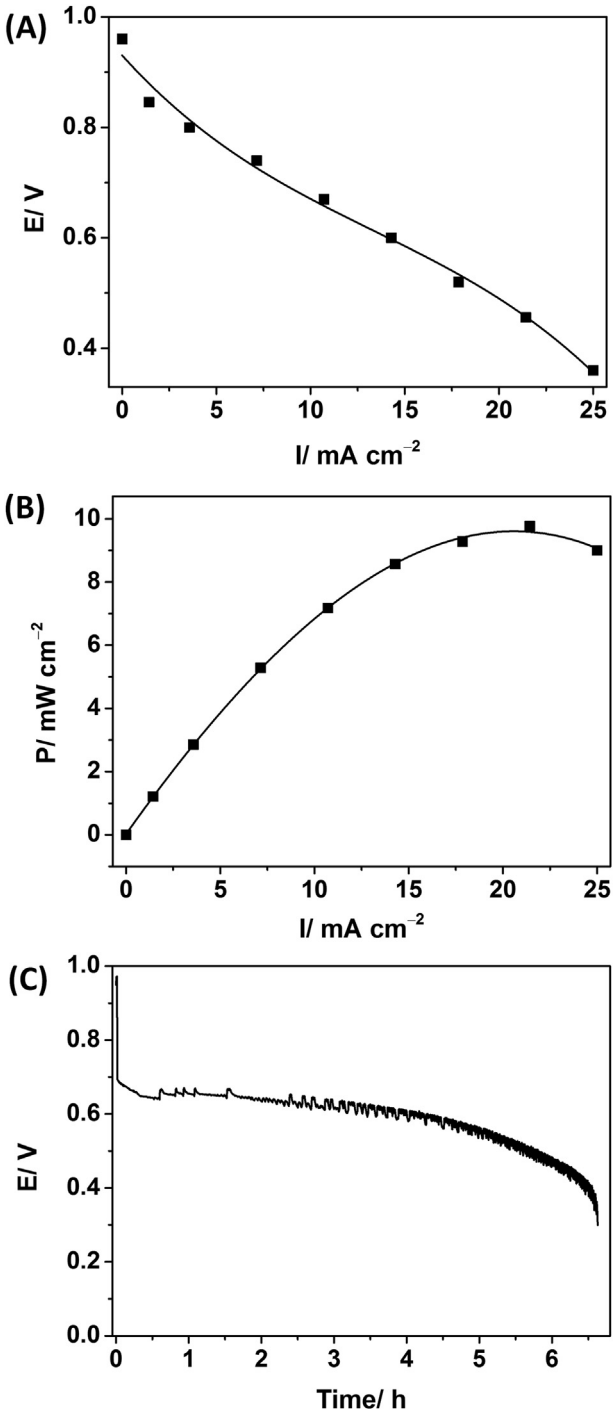

Fig. 7. (A) E vs. I curve for the hydrazine/air fuel cell (70 cm^2, 100 mL volume), corresponds to Fig. 5. (B) P vs. I curve derived. (C): Complete discharge at 1 A (14.3 mA cm^{-2}). Anodic solution: 3% hydrazine in 5.5 M KOH, 100 mL.

cell provides about 0.58 V at 1 A (14.3 mA cm^{-2}), and the discharge efficiency is about 70%.

Our Cu–Ni-hydrazine/air fuel cell produces lower OCP than the state-of-the art hydrazine/oxygen fuel cell, based on nano-Pt/carbon catalyst, used both as anode and cathode, and pure oxygen as oxidant (flow rate of 400 mL min^{-1}), as reported by Yamada et al. [32]. Notably, our fuel cell uses air (not pure oxygen), and no air pump is required for its effective operation. In addition, our non-noble metal hydrazine/air fuel cell is significantly simpler, and of dramatically lower cost when compared to the Pt-hydrazine/oxygen fuel cell.

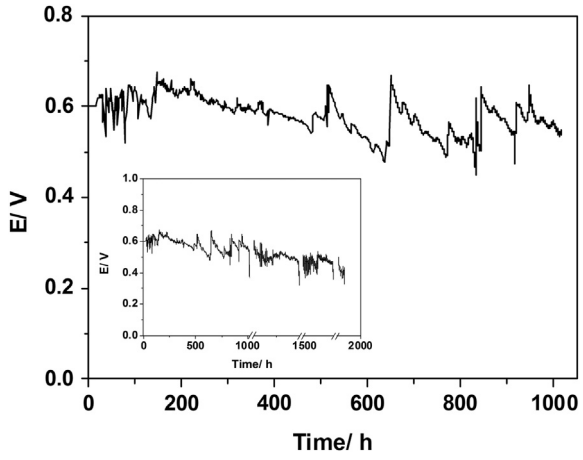

Fig. 8. Full discharge at 1 A (14.3 mA cm^{-2}) of the hydrazine/air fuel cell (70 cm^2, 100 mL volume). The fuel cell was operated with continuous flow (20 mL min^{-1}) of fuel solution (3% hydrazine in 5.5 M KOH). Inset: cell under longer operation times. Potential spike irregularities are due to times where cell maintenance was performed.

This hydrazine/air fuel cell assembly was operated at 1 A (14.3 mA cm^{-2}) with continuous flow of the fuel solution (20 mL min^{-1} of 3% hydrazine in 5.5 M KOH). This fuel cell operates for more than 1000 h, as seen in Fig. 8, and supplies about 0.58 V at 1 A (14.3 mA cm^{-2}). The discharge efficiency corresponds to approximately 70%. During the discharge process the potential of the Cu–Ni anode was in a range between −1.0 to −0.9 V (vs. Ag/AgCl), while the potential of the air-cathode was in a range between −0.3 V to −0.5 V (vs. Ag/AgCl). Also, we found before that the air cathode losses its activity in the presence of high concentrations of hydrazine (above 10%). Thus, the use of a stable anion exchange membrane in the new construction (Fig. 6) is essential for achieving long time operation of our fuel cell. In addition, the use of commercial anion exchange membranes, combined with newly-added the KOH-solution chamber (about 5 mm thick), increases the fuel cell resistance (slightly decreasing its power as compared to our previous study [36]), but allowing its long time operation.

4. Conclusion

We have developed a new room-temperature hydrazine/Air direct-liquid fuel cell based on a *nanotextured* bimetallic Cu–Ni anode, used as hydrazine catalyst. The Cu–Ni/hydrazine anode shows high catalytic activity for extended periods of continuous operation. The surface decoration of *nanotextured* Cu anodes with trace amounts of Ni leads to a substantial current density improvement, without negatively affecting the catalyst electrochemical efficiency due to potentially increased non-electrochemical degradation of the hydrazine by the nickel deposited traces. These important findings suggest that a new generation of improved catalyst electrodes may be envisioned by the simple optimized combination of multiple metals in a single electrode. In addition, a new cell design was developed, leading to an improved hydrazine/air fuel cell, able to reliably operate for nearly 2000 h, Fig. 8 inset, providing about 0.58 V at 1 A (14.3 mA cm^{-2}). The discharge efficiency corresponds to about 70%.

Acknowledgments

We gratefully acknowledge Nanergy Ltd for the financial support.

References

[1] G.H. Miley, N. Luo, J. Mather, R. Burton, G. Hawkins, L. Gu, E. Byrd, R. Gimlin, P.J. Shrestha, G. Benavides, J. Laystrom, D. Carroll, J. Power Sources 165 (2007) 509–516.

[2] B.C.H. Steele, A. Heinzel, Nature 414 (2001) 345–352.
[3] N.Q. Minh, J. Am. Ceram. Soc. 76 (1993) 563–588.
[4] O. Yamamoto, Electrochim. Acta 45 (2000) 2423–2435.
[5] L. Carrette, K.A. Friedrich, U. Stimming, Chem. Phys. Chem 1 (2000) 162–193.
[6] U.B. Demirci, J. Power Sources 169 (2007) 239–246.
[7] M. Winter, R.J. Brodd, Chem. Rev. 104 (2004) 4245–4270.
[8] R. Parsons, T. Vandernoot, J. Electroanal. Chem. 257 (1988) 9–45.
[9] L. Carrette, K.A. Friedrich, U. Stimming, Fuel Cells 1 (2000) 5–39.
[10] V. Mehta, J.S. Cooper, J. Power Sources 114 (2003) 32–53.
[11] S. Pandiyan, A. Elayaperumal, N. Rajalakshmi, K.S. Dhathathreyan, N. Venkateshwaran, Renewable Energy 49 (2013) 161–165.
[12] H. Liu, C. Song, L. Zhang, J. Zhang, H. Wang, D.P. Wilkinson, J. Power Sources 155 (2006) 95–110.
[13] S. Wasmus, A. Kuver, J. Electroanal. Chem. 461 (1999) 14–31.
[14] X. Ren, P. Zelenay, S. Thomas, J. Davey, S. Gottesfeld, J. Power Sources 86 (2000) 111–116.
[15] K.D. Kreuer, J. Membr. Sci. 185 (2001) 29–39.
[16] X. Ren, M.S. Wilson, S. Gottesfeld, J. Electrochem. Soc. 143 (1996) L12–L15.
[17] N.A. Choudhury, R.K. Raman, S. Sampath, A.K. Shukla, J. Power Sources 143 (2005) 1–7.
[18] C. Ponce de León, F.C. Walsh, A. Rose, J.B. Lakeman, D.J. Browning, R.W. Reeve, J. Power Sources 164 (2007) 441–448.
[19] S.C. Amendola, P. Onnerud, M.T. Kelly, P.J. Petillo, S.L. Sharp-Goldman, M. Binder, J. Power Sources 84 (1999) 130–133.
[20] R.K. Raman, A.K. Shukla, Fuel Cells 3 (2007) 225–231.
[21] C. Ponce de León, F.C. Walsh, D. Pletcher, D.J. Browning, J.B. Lakeman, J. Power Sources 155 (2006) 172–181.
[22] J.-H. Wee, J. Power Sources 155 (2006) 329–339.
[23] X.-B. Zhang, S. Han, J.-M. Yan, M. Chandra, H. Shioyama, K. Yasuda, N. Kuriyama, T. Kobayashi, Q. Xu, J. Power Sources 168 (2007) 167–171.
[24] X.-B. Zhang, S. Han, J.-M. Yan, H. Shioyama, N. Kuriyama, T. Kobayashi, Q. Xu, Int. J. Hydrogen Energy 34 (2009) 174–179.
[25] C. Yao, H. Yang, L. Zhuang, X. Ai, Y. Cao, J. Lu, J. Power Sources 165 (2007) 125–127.
[26] X.-B. Zhang, J.-M. Yan, S. Han, H. Shioyama, K. Yasuda, N. Kuriyama, Q. Xu, J. Power Sources 182 (2008) 515–519.
[27] U.B. Demirci, P. Miele, Energy Environ. Sci. 2 (2009) 627–637.
[28] B. Filanovsky, E. Granot, R. Dirawi, I. Presman, I. Kuras, F. Patolsky, Nano Lett. 11 (2011) 1727–1732.
[29] G.E. Evans, K.V. Kordesch, Science 158 (1967) 1148–1152.
[30] A. Serov, C. Kwak, Appl. Catal. B Environ. 98 (2010) 1–9.
[31] S.J. Lao, H.Y. Qin, L.Q. Ye, B.H. Liu, Z.P. Li, J. Power Sources 195 (2010) 4135–4138.
[32] K. Yamada, K. Yasuda, H. Tanaka, Y. Miyazaki, T. Kobayashi, J. Power Sources 122 (2003) 132–137.
[33] K. Yamada, K. Asazawa, K. Yasuda, T. Ioroi, H. Tanaka, Y. Miyazaki, T. Kobayashi, J. Power Sources 115 (2003) 236–242.
[34] K. Asazawa, K. Yamada, H. Tanaka, A. Oka, M. Taniguchi, T. Kobayashi, Angew. Chem. Int. Ed. 46 (2007) 8024–8027.
[35] K. Yamada, K. Yasuda, N. Fujiwara, Z. Siroma, H. Tanaka, Y. Miyazaki, T. Kobayashi, Electrochem. Commun. 5 (2003) 892–896.
[36] B. Filanovsky, E. Granot, I. Presman, I. Kuras, F. Patolsky, J. Power Sources 204 (2012) 116–121.
[37] N.V. Korovin, B.N. Yanchuk, Electrochim. Acta 15 (1970) 569–580.
[38] G.-W. Yang, G.-Y. Gao, C. Wang, C.-L. Xu, H.-L. Li, Carbon 46 (2008) 747–752.
[39] B. Seger, P.V. Kamat, Phys. Chem. C 113 (2009) 7990–7995.
[40] Q. Yi, L. Li, W. Yu, Z. Zhou, G. Xu, J. Mol. Catal. A Chem. 295 (2008) 34–38.
[41] J. Sanabria-Chinchilla, K. Asazawa, T. Sakamoto, K. Yamada, H. Tanaka, P. Strasser, J. Am. Chem. Soc. 133 (2011) 5425–5543.
[42] W.X. Yin, Z.P. Li, J.K. Zhu, H.Y. Qin, J. Power Sources 182 (2008) 520–523.
[43] K. Asazawa, T. Sakamoto, S. Yamaguchi, K. Yamada, H. Fujikawa, H. Tanaka, K. Oguro, J. Electrochem. Soc. 156 (2009) B509–B512.
[44] A. Upton, N. Johnson, J. Sandy, E. Sim, Trends Pharmacol. Sci. 22 (2001) 140–146.
[45] F. Patolsky, B. Filanovsky, E. Granot, PA WO/2010/055511.
[46] H.-C. Shin, M. Liu, Chem. Mater. 16 (2004) 5460–5464.
[47] S.Y. Grilikhes, K.I. Tichonov, in: Khimia (Ed.), Electochemistry and Chemistry Plating, 1990, pp. 168–172. Saint Petersburg Russia.
[48] B. Zhao, J. Song, R. Ran, Z. Shao, Int. J. Hydrogen Energy 37 (2012) 1133–1139.
[49] S.K. Singh, X.-B. Zhang, Q. Xu, J. Am. Chem. Soc. 131 (2009) 9894–9895.
[50] S.K. Singh, Q. Xu, J. Am. Chem. Soc. 131 (2009) 18032–18033.